Spatiotemporal drivers of food system GHG emissions in China

Article

Accepted Version

Qi, X., Huang, X., Zhong, H., Thompson, J. R., Yang, H. ORCID: https://orcid.org/0000-0001-9940-8273, Zhong, T. and Peng, X. (2024) Spatiotemporal drivers of food system GHG emissions in China. Resources, Conservation and Recycling, 205. 107580. ISSN 1879-0658 doi: 10.1016/j.resconrec.2024.107580 Available at https://centaur.reading.ac.uk/115974/

To link to this article DOI: http://dx.doi.org/10.1016/j.resconrec.2024.107580

Publisher: Elsevier

Spatiotemporal drivers of food system GHG emissions in China

Xinxian Qi [1,2], Xianjin Huang[1,2]*, Honglin Zhong [3], Julian R. Thompson[4], Hong Yang[5]*, Taiyang Zhong[1], Xu Peng[6]

1. School of Geography and Ocean Science, Nanjing University, Nanjing, Jiangsu 210023, China
2. The Key Laboratory of Carbon Neutrality and Territory Optimization, Ministry of Natural Resources, Nanjing, Jiangsu 210023, China
3. Institute of Blue and Green Development, Shandong University, Weihai 264209, China
4. Department of Geography, University College London, London WC1E 6BT, UK.
5. Department of Geography and Environmental Science, University of Reading, Reading RG6 6AB, UK.
6. School of Business, Jiangnan University, Wuxi, 214122, China

*Corresponding authors:
hxj369@nju.edu.cn (X. H.), h.yang4@reading.ac.uk (H. Y.)

Abstract: Food systems emissions (FSE) account for one-third of anthropogenic GHGs. Mitigating these emissions is pivotal for achieving the 1.5°C target. Given current research gaps in regional FSE accounting and drivers for China, the world's largest food system emitter, this study constructs a regionally specific, bottom-up FSE inventory detailed by food types and downscales FSE drivers to the provincial level. China's FSE exhibited an initial decline due to energy pattern upgrades during the period of 1990–2000, followed by a rise between 2000 and 2018. Increases were predominantly in developed southern regions and were propelled by economic growth, consumer expenditure, and dietary pattern shifts. This study reveals the spatial heterogeneity of emission sources and drivers, emphasizing the necessity of demand-side mitigation strategies in developed areas. It underscores the importance of formulating regionally differentiated emission reduction and interregional compensation policies.

Keywords: food system, GHG emissions, spatial heterogeneity, drivers, mitigation

1. Introduction

The entire food system (production, processing, distribution, preparation and consumption) accounts for approximately one-third (34% [25-42%]) of total anthropogenic greenhouse gases (GHGs) (Crippa et al., 2021; Rosenzweig et al., 2020). Recent studies have revealed the increasing dominance of GHG emissions from pre-and post-production processes along supply chains (Tubiello et al., 2022). China is the world's largest food system carbon emitter (Godfray et al., 2018). It covers a vast territory that is characterized by heterogeneous environmental and socioeconomic conditions and is currently transitioning to high-quality diets (He et al., 2018; Zhao et al., 2021). Although the estimated food system emissions (FSE) per capita from China's food system are still far below the global average (Crippa et al., 2021), the nation's food system is facing profound mitigation pressure to meet future demands (Zhao et al., 2021) in the context of the 2060 carbon neutrality goal and 1.5°C global warming targets (Acampora et al., 2023; Roe et al., 2019; Yang et al., 2022). FSE are also distributed unequally at both national (Poore and Nemecek, 2018) and regional scales (Xing et al., 2023), producing inequality in these mitigation pressures (Sun et al., 2021). Identification of the spatial distributions of FSE and their driving forces is urgently required to develop regional-specific mitigation strategies for the food sector.

The drivers of food-related GHG emissions, alongside measures through which they can be reduced, are related to both the demand- and supply-sides of the food system (Godfray et al., 2010; Poore and Nemecek, 2018). On the one hand, supply-side GHGs emissions can be reduced by closing the yield gap (Zhang et al., 2013), promoting sustainable intensification (Chen et al., 2014), and developing efficient management practices (Bajželj et al., 2014; Ren et al., 2023). On the other hand, food-related emissions largely depend on sustainable healthy diets (Heller and Keoleian, 2015; IPCC, 2022) and food loss and waste (Li et al., 2021; Xue et al., 2021) from the demand-side. These are influenced by dietary patterns and preferences (Hayek et al., 2021; He et al., 2018; He et al., 2021), food prices (Fujimori et al., 2022; Kehlbacher et al., 2016) and consumption expenditure (Kramer et al., 1999). Decomposition methods have been used to detect the drivers of FSE (Schierhorn et al., 2019). For example, He et al. (2018) decomposed dietary-driven GHG emissions into seven factors: aging, calorie intake, energy structure, nutrient composition, population growth, technical progress, and urbanization. Cerutti et al. (2023) identified three additional drivers: per capita GHG emissions, land intensity, and emissions intensity. However, the current detection of drivers is primarily at the national scale and there is a general absence of detailed regional information to examine spatial patterns that influence FSE (Huang et al., 2020). Mitigation of food system GHG emissions should address both demand and supply sides with regional specifics, but such an integrated approach is currently lacking in China.

Despite significant heterogeneity in the patterns of FSE, particularly at the production stage due to diverse commodity production and varying production efficiencies (Poore and Nemecek, 2018; Rosenzweig et al., 2020), targeted mitigation policies remain a challenge. Hong et al. (2021) decomposed emission drivers related to land-use at the national level, underscoring the importance of regionally differentiated mitigation strategies. This spatial heterogeneity is also evident on the demand side with Sun et al. (2022) revealing that dietary shifts in developed regions possess higher emission reduction potential. Nevertheless, in China, a country typified by significant food production and consumption (Zhang et al., 2022), natural resource endowment and economic development are unevenly distributed (Qiang and Jian, 2020), inevitably leading to regional disparities in FSE and their drivers (Qi et al., 2023). Furthermore, the concentration of China's population and economy in the south, coupled with the northward shift of cropland and production, is likely to exacerbate the spatial imbalances in FSE (Qi et al., 2022). While some studies have explored region-specific socioeconomic drivers of agricultural methane emissions (Duan et al., 2023) and nitrogen use (Gao et al., 2019) in China, the drivers of regional life-cycle FSE remain unidentified. This knowledge gap hampers the ability of policymakers to devise and implement effective and targeted food system mitigation policies.

To address knowledge gaps regarding region-specific GHGs accounting within China’s food system and to examine the regional drivers influencing food system emissions, this study aims to develop a lifecycle FSE inventory from farm to fork at the provincial level. Initially, our research uncovers the structural trends and spatial characteristics of FSE, detailing the contributions of various food types to emissions. Subsequently, we decompose the factors influencing the changes in China's food system GHGs and downscale these factors, providing insights with regional specificity. Furthermore, our study illuminates the coupling trends of food system emissions alongside their most influential drivers. The insights garnered from our findings are poised to aid policymakers in comprehending the features and spatial heterogeneity of China's food system emissions, thereby enabling the formulation of regionally tailored strategies to food system GHGs emission reduction.

2. Material and methods

2.1 System boundary of "bottom-up" GHGs inventory

The food system paradigm breaks down entrenched sectoral categories either following the Intergovernmental Panel on Climate Change (IPCC) or the United Nations Framework Convention on Climate Change (UNFCCC) GHG emissions inventory guidelines (Rosenzweig et al., 2020) and by categorizing elements of the former "agriculture, forestry, and other land use" (AFOLU) sector. Derived and developed largely from food supply chain concepts (Garnett, 2011), the food system primarily encompasses land use and land cover change (LULCC), production, transport, processing, packaging, retail, consumption, and waste disposal (EU, 2020; Crippa et al., 2021).

The food system assessed in this study involves 12 primary food categories consumed by Chinese people and comprises five plant-sourced foods (rice, wheat, maize, vegetables, and fruit), seven animal-sourced foods (pork, beef, mutton, poultry, egg, and milk), and aquatic foods (fish, shrimp, crab, shellfish, and algae). The nutrients supplied from these 12 food categories account for 85.4% of the total calories and 88.7% of protein intake by Chinese people (FAOSTAT, 2023). Following the EU (2020) Farm-to-Fork Strategy, the food supply chain includes preproduction (extraction of the resources needed to produce agricultural products), production (the land and farm management practices by farmers during the food production process), and post-production (processing, transportation, packaging, distribution, retail, household refrigeration and cooking).

For plant-sourced foods, the food supply chain begins with the pre-production extraction of resources needed to produce inputs for agricultural production, such as energy products including coal, diesel and electricity, and agricultural materials and products including plastic film, seeds, pesticides and N/P/K fertilizers. The production stage includes machinery diesel use for seeding, harvesting and other farming activities, electricity for irrigation, CH_4 emissions from paddy cultivation and straw burning, as well as direct and indirect N_2O emissions from fertilizers. Emissions induced by land use change (agricultural land expansion, forest burning, organic soil burning), human labor, the manufacture of agricultural equipment, and the construction of farm buildings are excluded in this study.

For animal-sourced foods, the food supply chain begins with the pre-production forage planting and processing, with emission factors derived from processed forage crops such as maize, soybean, and wheat. There are three main emissions sources for the animal-sourced food production: farm energy, ruminant animal fermentation, and manure management. Emissions caused by farm infrastructure construction, grassland nitrogen fixation and loss, and manual labor are not considered in this study.

Both the plant-sourced and animal-sourced foods have the same post-production stages (processing, transportation, packaging, distribution, retailing), and they both end at household refrigeration and cooking. Emissions from LULUC associated with agriculture in the preproduction stage are excluded from the assessment due to the challenges in directly linking them to the food lifecycle, which is the fundamental framework employed in this study (Lai et al., 2016). Post-consumption stages (food waste and disposal) are not considered owing to their high variability and low food-specific data availability (Xue et al., 2021). Additionally, this study only considers emission processes within each region’s borders; emissions transfer associated with food trade between regions and countries are excluded.

2.2 Carbon emission accounting of the food system

Building upon given system boundaries, food system carbon emissions accounting can be categorized into two main methodologies. The first type stems from a top-down sectoral breakdown. This includes estimates from the NASA Research Institute (Rosenzweig et al., 2020), the Food and Agriculture Organization (FAO) (Tubiello et al., 2021), the EU Joint Research Center (Crippa et al., 2021), the CAAS (Zhang et al. 2021), and CAS (Liu et al., 2023). These sources have been instrumental in tracking trends and shifts in global food system sectoral GHG emissions, and demonstrate the increasing prominence of GHG emissions in both pre-production and post-production stages across supply chains. This provides a consistent and transparent framework for national level accounting. However, there is a notable lack of region-specific and food type-specific emission inventories, which are critical for developing targeted mitigation strategies. The second methodological category employs a bottom-up life cycle analysis (Poore and Nemecek, 2018), advantageous for its emissions inventory that encompasses various food types throughout their entire life cycle stages. This approach facilitates the identification of primary emission sources and measurement units. Given this study's focus on the impact of food consumption patterns on emissions, a bottom-up life cycle analysis is the preferred method.

Life Cycle Assessment (LCA) is the evaluation of the environmental burdens associated with a product, process, or activity. It is based on identifying and quantifying the energy and materials used and, in turn, the waste materials released into the environment (Garnett, 2011). The International Organization for Standardization (ISO) has standardized this framework within the ISO 14040 series on LCA. The LCA of the food system includes the entire lifecycle of food, encompassing preproduction, production and post-production processes. Consumption-based food system emissions in China are accounting as formulas below:

$$FSE_{i,j} = \sum_{k} EF_{i,j,k} * A_{i,j} \qquad \text{Equation 1}$$

where i represents the food type consumed, j represents the consumption region in this case one of 31 provinces in mainland China (Hongkong, Macau, and Taiwan are excluded), k represents the food system stages of the lifecycle. $FSE_{i,j}$ represents consumption-based food system emissions of food type i in region j. $EF_{i,j,k}$ represents the emission factor of food type i in region j at lifecycle stage k. $A_{i,j}$ is activity data in LCA, represents total consumption amount of food type i in region j.

2.3 Framework for factors influencing food system GHGs

In order to explore the influencing factors of food system carbon emissions, we constructed a driving force framework that affected food system emissions from three categories (Fig. 1): (1) Supply side factors reflecting technology and management, incduing specific production practice and energy use pattern. In this study, we combined the lifecycle carbon intensity with diversified production practices and energy use into one technology factor. (2) Demand side factors such as consumption structure, price, Engel coefficient, and expenditure, and (3) Socio-economic factors including economic growth, urbanization and population.

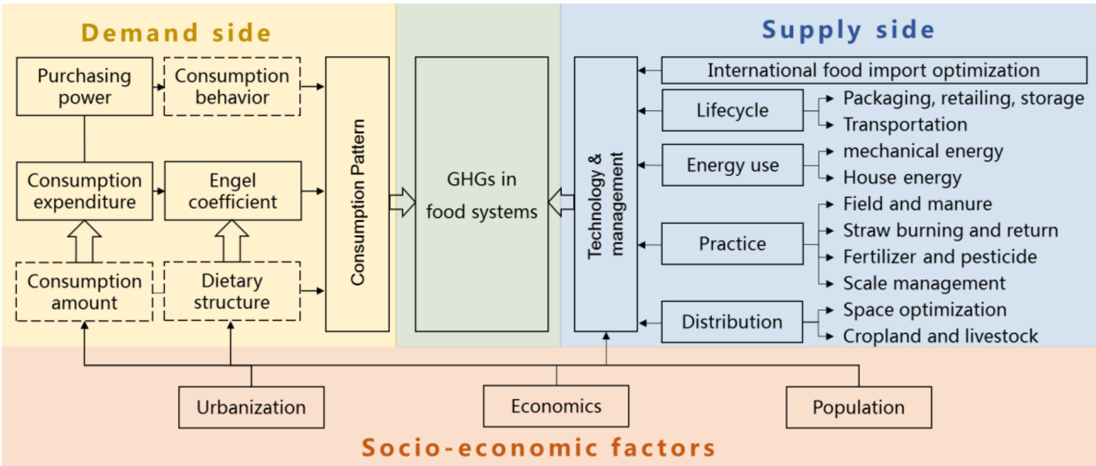

Figure 1. Framework of mechanisms influencing GHGs emissions from the food system in China.

2.4 LMDI decomposition analysis

The Log Mean Divisia Index (LMDI) method, developed by Ang (2004), was used to analyze how supply- and demand-side drivers affect food system

GHGs structural shifts in China. LMDI quantifies the contribution of each driving force in proportion without residuals. To conduct the decomposition analysis, the GHG changes for the different food types in each region were decomposed into eight factors: technology, food consumption structure, food purchasing power, Engel coefficient, expenditure, economic development, urbanization and population.

$$FE_{Total} = FE_U + FE_R \qquad \text{Equation 2}$$

$$\begin{aligned} FE_U = \sum_{i,j} \frac{FE_{U.i,\mathrm{j}}}{Con_{U,i,j}} \times \frac{Con_{U,i,j}}{Con_{U,j}} \times \frac{Con_{U,j}}{FEXP_{U,j}} \times \frac{FEXP_{U,j}}{EXP_{U,j}} \\ \times \frac{EXP_{U,j}}{GDP_{U,j}} \times \frac{GDP_{U,j}}{P_{U,j}} \times \frac{P_{U,j}}{P_j} \times P_j \\ = \sum_{i,j} EI_{U,i,j} \times DP_{U,i,j} \times CP_{U,j} \times EN_{U,j} \\ \times CE_{U,j} \times EG_{U,j} \times UR_{U,j} \times P_j \end{aligned} \qquad \text{Equation 3}$$

$$\begin{aligned} FE_R = \sum_{i,j} \frac{FE_{R.i,\mathrm{j}}}{Con_{R,i,j}} \times \frac{Con_{R,i,j}}{Con_{R,j}} \times \frac{Con_{R,j}}{FEXP_{R,j}} \times \frac{FEXP_{R,j}}{EXP_{R,j}} \\ \times \frac{EXP_{R,j}}{GDP_{R,j}} \times \frac{GDP_{R,j}}{P_{R,j}} \times \frac{P_{R,j}}{P_j} \times P_j \\ = \sum_{i,j} EI_{R,i,j} \times DP_{R,i,j} \times CP_{R,j} \times EN_{R,j} \\ \times CE_{R,j} \times EG_{R,j} \times UR_{R,j} \times P_j \end{aligned} \qquad \text{Equation 4}$$

where *i* denotes the different food types, *j* denotes the different provinces in mainland Chinese, *U* denotes urban factors, and *R* denotes rural factors. FE_{Total} are the total GHGs emissions from the food system in China (million tons CO_2e), and FE_U and FE_R are the GHGs from urban and rural residential consumption, respectively. $FE_{U.i,\mathrm{j}}$ denotes the urban residential consumption GHGs of food *i* in province *j*, $Con_{U,i,j}$ denotes the urban residential consumption weight of food *i* in province *j* (million tons), $Con_{U,j}$ denotes the urban residential consumption weight of all food types in province *j*, $FEXP_{U,j}$ is the food consumption expenditure of all types of food in province *j* (billion yuan), $EXP_{U,j}$ is the residential consumption expenditure in province *j* (billion yuan), $GDP_{U,j}$ represents the GDP from urban areas in province *j* (billion yuan), $P_{U,j}$ represents the urban population in province *j* (million person),, and P_j is the total population in province *j*. $EI_{U,i,j} = \frac{FE_{U,i,j}}{Con_{U,i,j}}$ represents the emission intensity from the entire food supply chain of food *i* in province *j*'s urban residential consumption (kg CO_2e kg^{-1}); $DP_{U,i,j} = \frac{Con_{U,i,j}}{Con_{U,j}}$ denotes the dietary pattern of food *i* in province *j*'s urban residential consumption (%); $CP_{U,j} = \frac{Con_{U,j}}{FEXP_{U,j}}$ denotes the purchasing power of all food types in province *j*'s urban residential consumption (which represents the reciprocal of food price) (kg/yuan); $EN_{U,j} = \frac{FEXP_{U,j}}{EXP_{U,j}}$ is the Engel coefficient of urban residents in province *j* (%); $CE_{U,j} = \frac{EXP_{R,j}}{GDP_{R,j}}$ is the consumption expenditure of urban residents in province *j* (%); $ES_{U,j} = \frac{GDP_{U,j}}{P_{U,j}}$ is the economic development of urban area in province *j* (1000 yuan per person); and $UR_{U,j} = \frac{P_{U,j}}{P_j}$ represents the urbanization ratio of province *j* (%).

$$\begin{aligned} \triangle FE_U &= FE_U^T - FE_U^0 \\ &= \triangle FE_{U,EI} + \triangle FE_{U,DP} + \triangle FE_{U,CP} + \triangle FE_{U,EN} + \\ &\quad \triangle FE_{U,CE} + \triangle FE_{U,EG} + \triangle FE_{U,UR} + \triangle FE_{U,P} \end{aligned} \quad \text{Equation 5}$$

$$\begin{aligned} \triangle FE_R &= FE_R^T - FE_R^0 \\ &= \triangle FE_{R,EI} + \triangle FE_{R,DP} + \triangle FE_{R,CP} + \triangle FE_{R,EN} + \\ &\quad \triangle FE_{R,CE} + \triangle FE_{R,EG} + \triangle FE_{R,UR} + \triangle FE_{R,P} \end{aligned} \quad \text{Equation 6}$$

where FE_U^T and FE_U^0 represent the GHGs from urban residential consumption in period *T* and the baseline period, respectively. $\triangle FE_U$ denotes the change in GHGs from urban residential consumption between period *T* and the baseline period. $\triangle FE_{U,EI}$, $\triangle FE_{U,DP}$, $\triangle FE_{U,CP}$, $\triangle FE_{U,EN}$, $\triangle FE_{U,CE}$, $\triangle$

$FE_{U,ES}$, $\triangle FE_{U,UR}$, and $\triangle FE_{U,P}$ indicate the contributions from technology, food consumption structure, purchasing power, Engel coefficient, expenditure, economic growth, urbanization and population, respectively.

2.5 Decoupling analysis

The decoupling analysis can be used to understand the relation between food system emissions and economic growth (Wang and Su, 2020). Tapio decoupling analysis is stable and unaffected by changes in statistical dimension. They provide additional details about the decoupling state. According to this method, the decoupling elastic index between food system emission per capita and per capita GDP is shown by Eq. 7:

$$D_{FE,EG} = \frac{(FE^t - FE^{t-1})/FE^{t-1}}{(EG^t - EG^{t-1})/EG^{t-1}} \quad \text{Equation 7}$$

were $D_{FE,EG}$ represents the decoupling states between food system emission per capita and GDP per capita. According to the differences in elastic indexes, FE^t represents food system emission per capita in year t, EG^t represents per capita GDP in year t. A value of $D_{FE,EG} > 0$ denotes coupling status, while $D_{FE,EG} < 0$ denotes decoupling status.

2.6 Data sources

The data used in this study comprise cost-benefit survey data of agricultural products, food prices, residential consumption data, emission factors of various foods in different life cycle stages, economic and social statistics data (see Supplementary Table S1 for a description of these data). Input data for the production stage mainly come from the national agricultural cost-benefit survey data and include most kinds of food input in the production process (N-P-K fertilizer and agricultural plastic films, the dosage of seeds, the costs of manure, pesticides, fertilizer, fuel, and power, food consumption, and food production data). The expenditure of some types of food was divided by the price to obtain the consumption amount of the food. Due to limited data availability across comparable years and regions for fruits and vegetables in the National Compilation of Cost and Benefit Data of Agricultural Products, this study selected the average inputs of apple and oranges to calculate the agricultural input of fruit. Similarly, the average inputs of cabbage, radish and tomato were selected to calculate the agricultural input for vegetables.

The per capita consumption data for 12 food types (rice, wheat, maize, vegetables, fruits, pork, beef, mutton, poultry, eggs, milk and aquatic products) came from the Statistical Yearbook of China and the Statistical Yearbook of 31 provincial administrative units. The emission factor data was obtained from IPCC National GHG Emission Inventory 2006, Provincial GHG Inventory Compilation Guide 2011, Standardization Administration of China, public databases and published literature. For the emissions from electricity consumption for the period after 2006, the 31 provincial administrative units in China were divided into six regional power grids using the emission factors of the China regional power grid baseline and the annual emission reduction project published by the National Development and Reform Commission after 2006. For the period before 2006, energy emission factors were obtained from the Chinese Life Cycle Database (CLCD).

3. Results

3.1 Spatial–temporal trends of food system GHG emissions in China

China's consumption-based food system GHGs emissions fluctuated between different periods. It decreases between 1990 and 2000 but then increased up to 2018. Across the entire period of 1990–2018, total GHGs from the Chinese food system increased from 1.44 Gt CO_2e yr^{-1} (95% confidence interval (CI): 1.00-1.88 Gt CO_2e yr^{-1}) to 1.55 Gt CO_2e yr^{-1} (95% CI: 1.07-2.03 Gt CO_2e yr^{-1}) (Fig. 2a; see Supplementary S5), which is 11.7% of the total GHGs in China (see Supplementary S2 for the results comparison). China's consumption-based food system emissions have undergone profound structural shifts in the dietary pattern in their spatial distribution. GHGs from China's food system has shifted from cereal-dominated foods in 1990 to highly carbon-intensive and more diverse foods (i.e., meat and protein products) in 2018 (Fig. 2a). Specifically, emissions from cereals reduced from 66.0% of the total in 1990 to 28.6% in 2018, while rice dropped from the top source of GHGs from the food system to the second. Moreover, the carbon emission proportion from meat increased from 19.5% to 39.1%. Pork has been the leading and principal source of GHG emissions (Fig. 2a), increasing by 70.8% from 1990 to 2018 and accounting for 23.9% of total meat emission growth. Emissions from protein products including milk and eggs have increased from 2.1% to 5.8%, whilst those from aquatic products have grown from 2.3% to 8.5% (Fig. 2a).

Spatially, consumption-based GHG emissions from China's food system were primarily concentrated in the south. The contribution of the southern part of the country (here comprising four regions: EC-East China, SC-South China, CC-Central China, and SW-Southwest China) to the national total GHGs decreased slightly from 77.0% in 1990 to 75.4% in 2018 (Fig. 2b). Total GHGs emissions from the food system in East China were the highest, accounting for 30.3% of the total national emissions, followed by South China with 16.0%. In contrast, Northwest China accounted for the lowest, only 6.1% in 2018 (Fig. 2b). In terms of the change rate between 1990 and 2018, GHGs from food systems increased in both the southern and northern regions, but the latter experienced a more rapid growth rate. On average, growth in the north was 15.2%, compared 6.2% in the south. Northwest China (NC) had the most rapid growth rate (68.8%), while Southwest (SW), Central (CC), and Northeast China (NE) experienced decreasing trends (3.5-6.7%) (Fig. 2b).

In terms of the spatial characteristics of GHGs emissions from different types of food, in most cases, with the exception of mutton, emissions from the south were higher than those from the north (Fig. 2b). From the perspective of dietary structural change, all regions showed a unified trend of decreasing GHGs emissions from cereal food and increasing emissions from fruit and vegetables, protein foods and aquatic products. However, there was significant spatial heterogeneity in emissions caused by regional dietary structure changes. Food system GHGs increases in South China were dominated by meat, those in North China were primarily from meat and vegetables, whilst those in East China were led by aquatic products (Fig. 2. c-f). As the largest food system GHGs emitter in the country, East China experienced the largest drop in cereal related emissions (-58.1%) and a large increase in meat (21.8%) and aquatic product (9.0%) emissions over the period of 1990–2018 (Fig. 2 c, f). In South China, high carbon-intensive meat consumption caused this region to experience the largest emission growth rate in the country. GHGs from meat consumption rose by the largest amount (219.4%), and the percentage of GHGs from meat increased from 19.0% in 1990 to 43.3% in 2018. In Northwest China, the large growth rate in food system GHGs emissions between 1990 and 2018 were dominated by meat (2.1 times) and vegetables (near doubling) (Fig. 2 c, f).

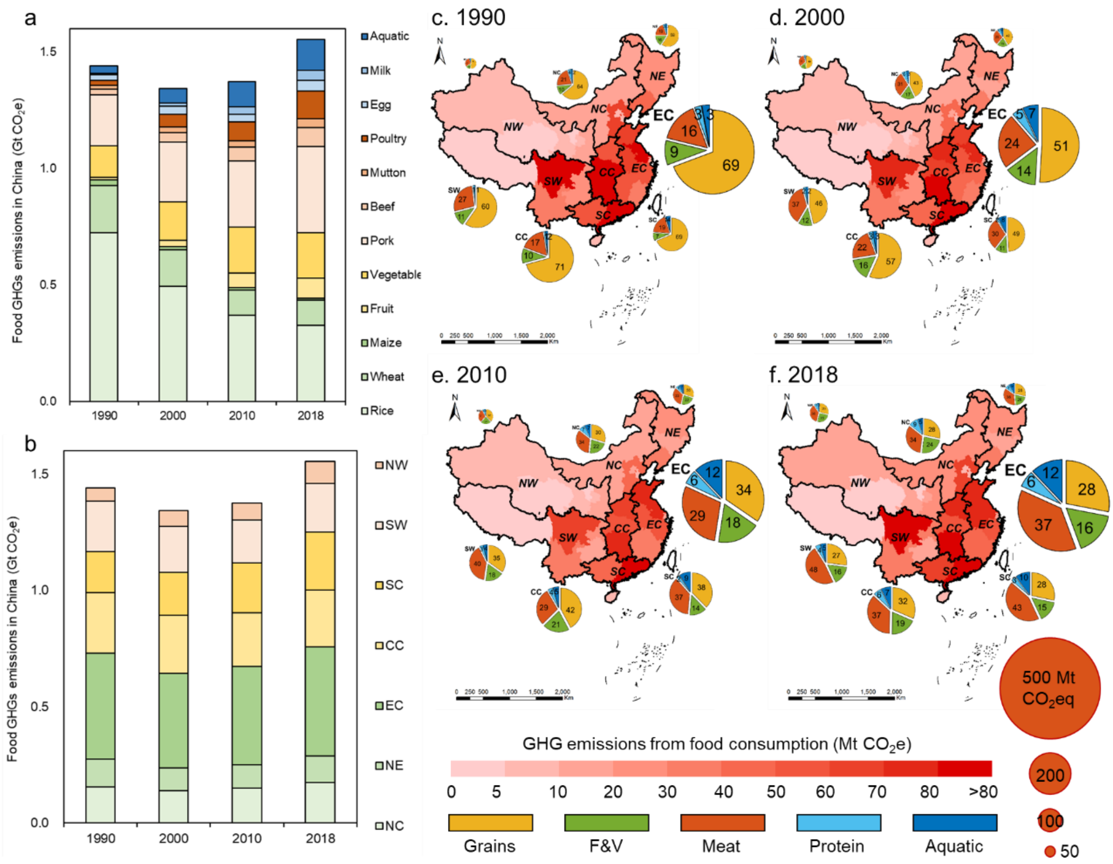

Figure 2. Spatial–temporal changes of China's food system emissions. a. China's total food system emissions related to food types; b. China's total food system emissions related to regions; c-f. represent the spatial distribution of food system emissions in China from 1990 to 2018. Different shades of red on the maps represent changes in total GHGs from regional food systems. Colors in the pie charts represent different food types with numbers representing percentages of the total. The sizes of pie charts correspond to emission amounts. Grains comprise rice, wheat, and maize; F&V comprise fruit and vegetables; meat comprises pork, beef, mutton, and poultry; protein comprises eggs and milk; and aquatic comprises fish, shrimp, crab, shellfish, and algae

etc. NE = Northeast China, NC = North China, NW = Northwest China, EC = East China, SC = South China, CC = Central China, and SW = Southwest China.

3.2 Drivers of food-related GHGs emissions at national level

To quantify the relative contributions of multiple drivers to total food system GHGs emissions, we used LMDI decomposition analysis to decompose the consumption-based GHGs changes for the different food types in each region into eight factors. These factors comprise one supply-side driver (technology), four demand-side drivers (food consumption structure, food purchasing power, Engel coefficient, and expenditure), and three socioeconomic drivers (economic growth, urbanization and population; Fig. 1). Overall, economic growth (contributing 173.2% of the growth) and food purchasing power (contributing 136.0% of the reduction) had the largest impacts on China's food system GHGs emission during the period of 1990–2018. The Engel coefficient contributed 57.8% to the decrease in GHGs emissions, whilst shifts in dietary pattern contributed 30.7% to the increase in these emissions. Changes in GHGs emission intensity contributed 28.4% of the decrease in food GHGs, while expenditure and population contributed 23.9% and 20.2% of the increases, respectively (Fig. 3). For the whole country, the impact of urbanization ratio was relatively small, with a cumulative impact of only 0.7%, but this does not represent the effects of urbanization-related dietary shifts, economic growth, and population changes. In addition, the influences of urbanization varied between different regions and different food types (for more details of the downscaling decomposition, see Fig. 6). The "supply-demand" factor decomposition model (Fig.1) was constructed to systematically analyze the influencing mechanisms driving changes in GHGs emissions from China's food system. Quantitative evidence from this analysis shows that the reduction effect caused by demand-side factors had a larger potential compared to supply-side factors (Table S3).

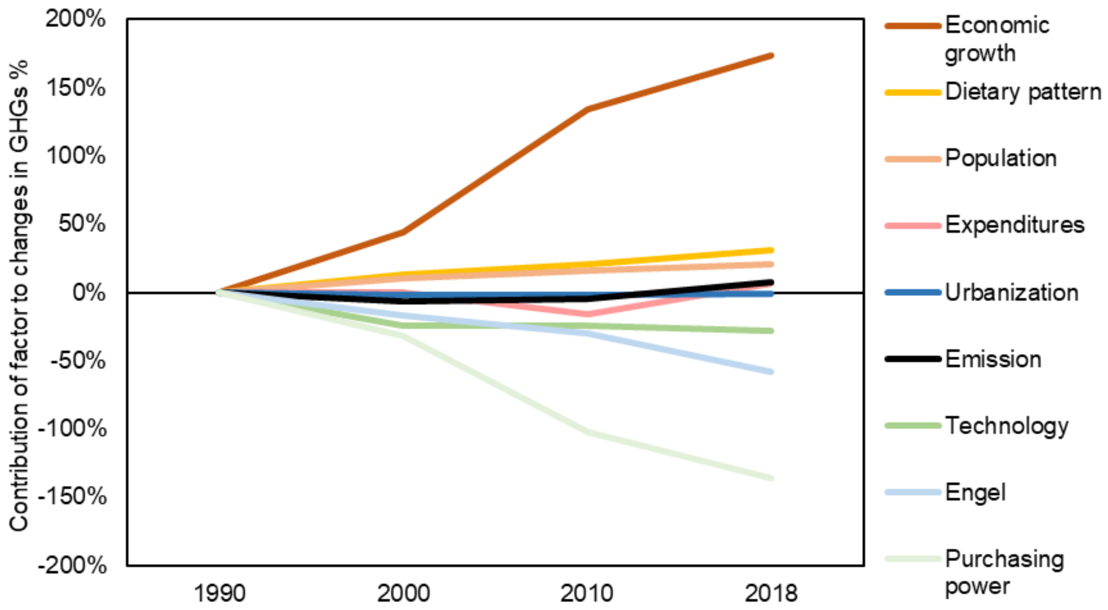

Figure 3. Contributions of different factors to changes in food system GHGs between 1990 and 2018. Using 1990 as the base year, the solid black line shows the percentage change in total food system GHGs. The other lines show the contribution to the change in emissions from eight different drivers.

Between 1990 and 2000 (P1), a period that was associated with achieving sufficient food for the Chinese people, GHGs emissions from China's food system decreased by 6.8% (Fig. 4). The reduction in emission intensity (technology) of 9.8% was the main reason for the overall reduction in food system GHGs during this period. Optimization of the energy structure of the food system in East, Central and Southwest China (Fig. 4, Fig. 5) resulted in reduced use of raw coal in the processing of cereal (e.g. wheat and maize) and rice. Economic growth, dietary pattern and population growth contributed 43.7%, 13.4% and 10.0% to the overall growth, respectively, while the Engel coefficient and food purchasing power contributed 16.6% and 31.7% to the decrease, respectively (Fig. 4). Food purchasing power contributed the most to the declines in East China for all food types.

During the period of 2000–2010 (P2), a stage associated with progress toward more comfortable standards of living for many Chinese people, the direction of change in China's food system GHGs reversed with overall increases, albeit of relatively small magnitude (2.3%, Fig. 4) taking place. Economic growth played the largest role in this period, contributing 96.9% of overall growth and being particularly important in East China, Central China, South China and Southeast China, (Fig. 4, Fig. 5). China's per capita gross domestic product (GDP) increased from 1,222 USD in 2000 to 4,740 USD in 2010, an almost 3-fold increase. Other increases were due to consumption structure transformation (7.4%), population growth (6.0%) and emission intensity (technology), although the influence of the latter weakened (0.7%) compared to the previous period. Reductions in consumption expenditure and food purchasing power contributed 17.0% and 75.8% to the decreases but these could not offset the growth brought about by the other drivers.

Between 2010 and 2018 (P3), a period with widespread comfortable living standards, GHGs emissions from China's food system continued to increase with an overall growth of 13.1% (Fig. 4). Transformation of consumer expenditure contributed 23.9% of the increase and was particularly concentrated in Central, East China, and North China (Fig. 5). The increasing effect of the transformation of the dietary pattern contributed 10.9% of the growth and was focused, in particular, within the developed areas in East, Central, Southwest, and South China (Fig. 4, Fig.5). A total of 86.6% of the emission increase by consumption structure was related to GHG-intensive consumption of meat, protein foods and vegetables (Fig. 4b). In addition, economic growth contributed 41.1% of the GHGs increase. While the reduction in GHGs from the food system due to the Engel coefficient increased to 29.4%, the food purchasing power effect on the reduction in food system GHGs decreased by 35.4%. The impacts of emission intensity (technology) on GHGs emission reductions declined in all regions and even reversed (i.e., increase in GHGs) in North and Northwest China (Fig. 5).

There were apparent spatial variations in the effects of the different drivers on food system GHGs emissions. The impacts of urbanization were relatively small (3.9% decrease overall) (Fig. 3) but continued to increase in Northwest and North China with the influence direction switching from decreases to increases in Northeast, East and South China (Fig. 5, Fig. 6). In particular, within the highly urbanized South and East China, the impacts of urbanization on food system GHGs emission decreased in the first two periods described above (1990–2000 and 2000–2011) then increased between 2010 and 2018. Increases in GHGs emissions driven by population gradually weakened in all regions, especially in Northeast China; in the final period, the population even had a decreasing effect (Fig. 5).

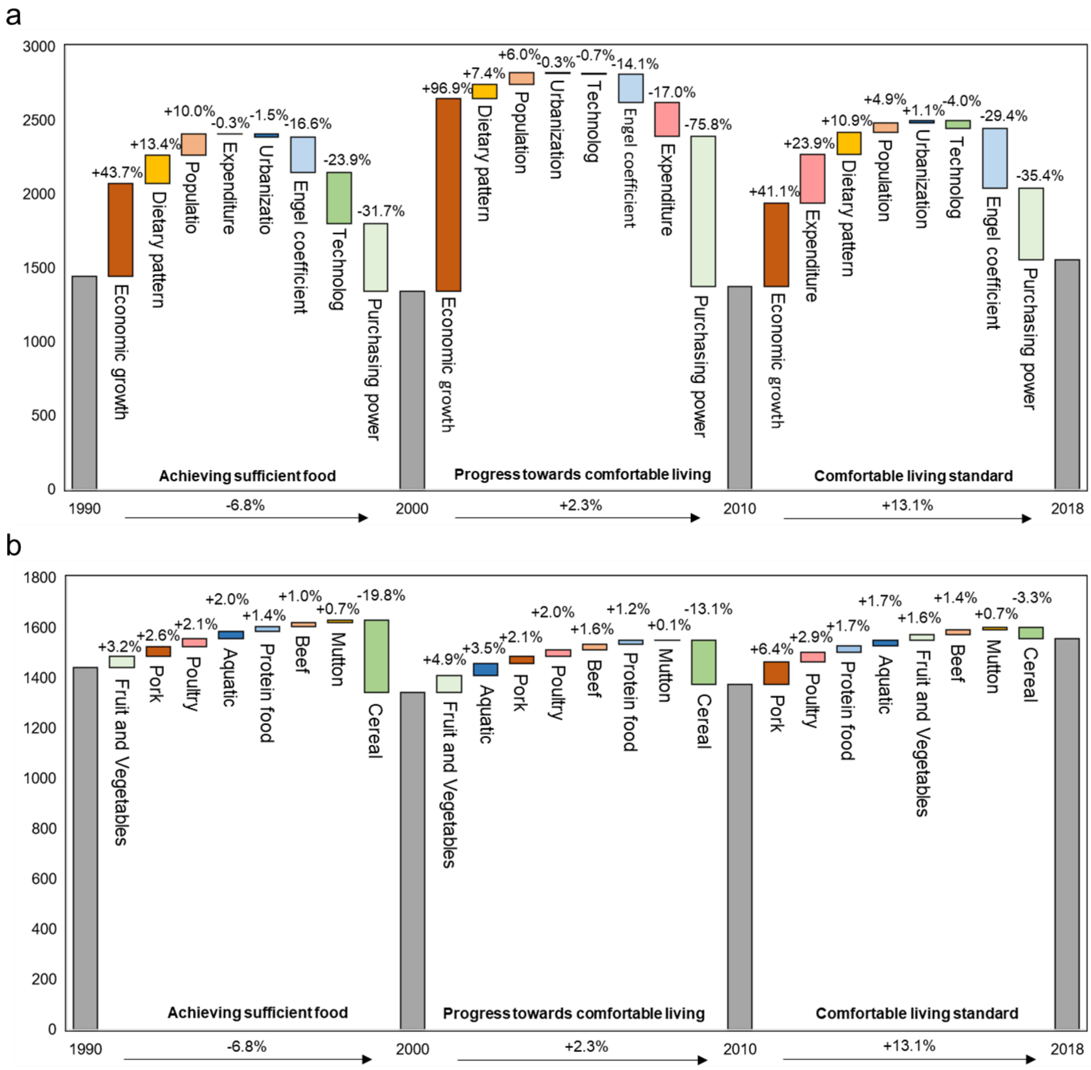

Figure 4. Contribution to the changes of GHGs from China's food system in three periods. a. Contribution of different factors of GHGs in food system in three periods. b. Contribution of different food types of GHGs in food system in three periods. According to the classification standard of the Engel coefficient used by the FAO these periods are 1990–2000 (P1) - achieve sufficient food, Engel's range 50%–59%; 2000–2010 (P2) – progress towards comfortable

standards of living, Engel's range 40%–49%; and 2010–2018 (P3) – widespread comfortable living standards, Engel's range 30%–39%.

3.3 Spatial heterogeneity of food-related GHGs emissions drivers

Different drivers not only have varying impacts and contributions to the consumption-based food system emissions (FSE), but their effects also demonstrate spatial heterogeneity, which provides evidence for the need to formulate regionally differentiated strategies for reducing FSE. Regionally, economic growth (EG) in southern regions including EC, SC, CC, and SW, contributes to approximately 78.5% of the increase in FSE. Within the southern regions, the EC has the largest contribution to economic growth effect, although its share of the national total economic contribution decreased from 36.6% in P1 to 31.4% in P3 (Fig. 5 a, b, c). Regarding purchasing power effects (CP), which make the largest overall contribution to emission reductions, the southern regions similarly contribute about 78.1% of the maximum emission reduction. Changes in purchasing power levels in EC contribute most significantly to this reduction, even though their share of the total national reduction in purchasing power contribution declined from 33.1% in P1 to 27.0% in P3 (Fig. 5a, b, c). Technological effects (EI) accounted for a 23.9% reduction in emissions during P1, with the transition away from coal in agricultural and livestock practices in southern regions contributing to 75.3% of technology effects (Fig. 5a). Consumer expenditure (CE) related to economic growth contributed to a 23.9% increase in emissions in P3, predominantly occurring in the EC, CC, and NC regions (Fig. 5c).

Regions are influenced by varying factors at different developmental stages, which in turn impact their FSE, indicating dynamic monitoring and regulation of these regional factors are essential for emission reduction. In P1, EC contributes most significantly to the reduction of food system emissions, primarily due to technology effects, expenditures, and the Engel coefficient (Fig. 5d). However, a weakening of its technology impact leads to EC contributing to an increase in food system emissions in P2 (Fig. 5e). In P3, heightened expenditures in EC accounts for the highest national contribution to FSE (Fig. 5f). SC demonstrates consistent growth in its contributions across all three phases, but the underlying factors driving this growth evolve, particularly as shifts in dietary patterns increasingly amplify SC's contributions (Fig. 5d, e, f).

The distribution of economic growth and purchasing power, both key drivers of FSE, was notably concentrated when disaggregated to the provincial level, as illustrated in Fig. 6. Additionally, a key factor contributing to the rise in emissions in P3 (i.e., 2010–2018) is the diminished mitigating impact of food purchasing power in southern regions. Similarly, the weakening of mitigation effects can also be attributed to a decrease in the contributions from technological advancements. During the period 1990–2000 (P1), regions such as Jiangsu, Anhui, Hubei, Hunan, and Sichuan, which benefited from technological advancements in emissions reduction, contributed approximately 25.6 Mt CO_2e each province to the reduction. However, there was a significant decrease of about 68.2% in these contributions during P3. Shifts in dietary patterns predominantly impacted southern regions, accounting for 86.6% of the national emission increase attributed to dietary changes in P3 (Fig. 6). Moreover, a substantial increase in total consumer expenditure in northern regions, especially in Hebei, Henan, and Liaoning, contributed to large emissions increases during P3, with an average of around 27.1 Mt CO_2e, alongside even larger increases of 37.2 Mt CO_2e in the southern region of Hunan. Changes in population growth had a pronounced effect on the southern regions, particularly Guangdong, which was alone responsible for 24.2% of the national emission increase attributed to population growth. However, across the whole period the overall contribution from population factors exhibited a gradual decline (Fig. 6).

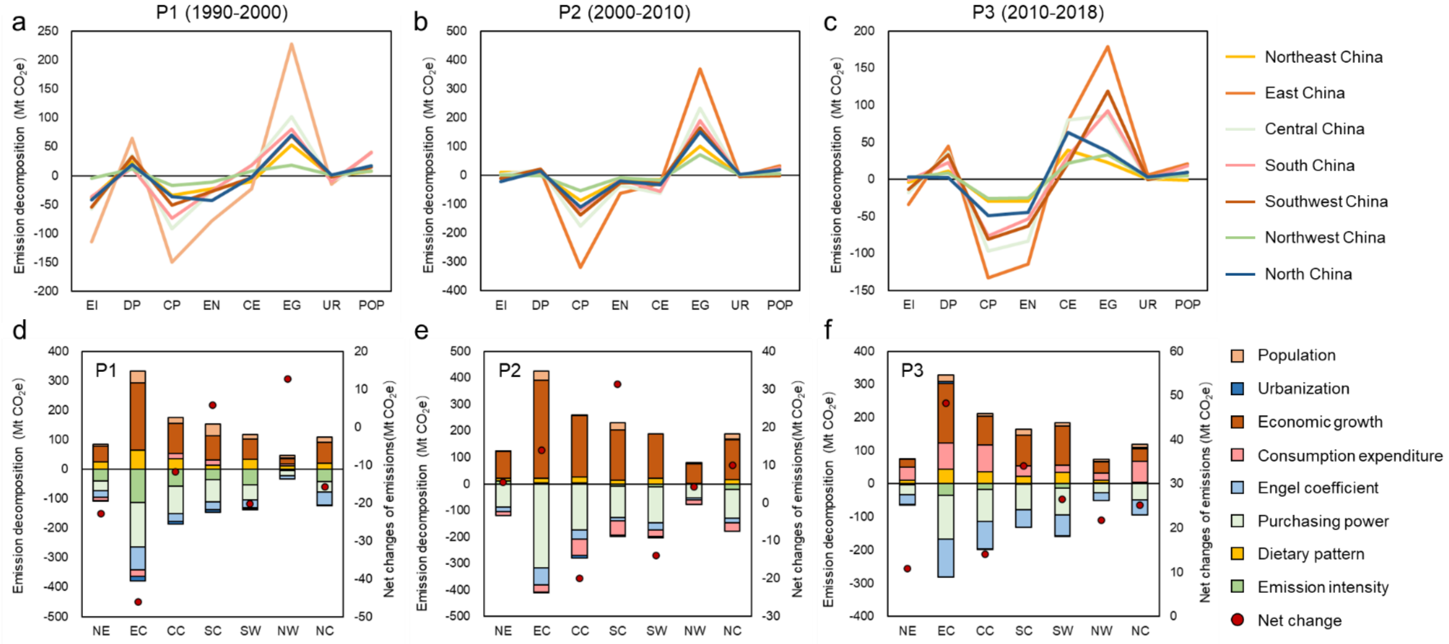

Figure 5 Change rate and decomposition of food system GHGs from seven regions in China. EI represents effects of technology, DP represents effects of dietary pattern, CP represents effects of purchasing power, EN represents effects of Engel coefficient, CE represents effects of consumption expenditure, EG represents effects of economic growth, UR represents effects of urbanization, POP represents effects of population. Parts a, b, c respectively represent the comparison of regional drivers in three periods. Parts d, e, f represent the decomposition results of regions in these periods respectively. P1 represents the period of 1990-2000, P2 represents the period of 2000-2010, and P3 represents the period of 2010-2018.

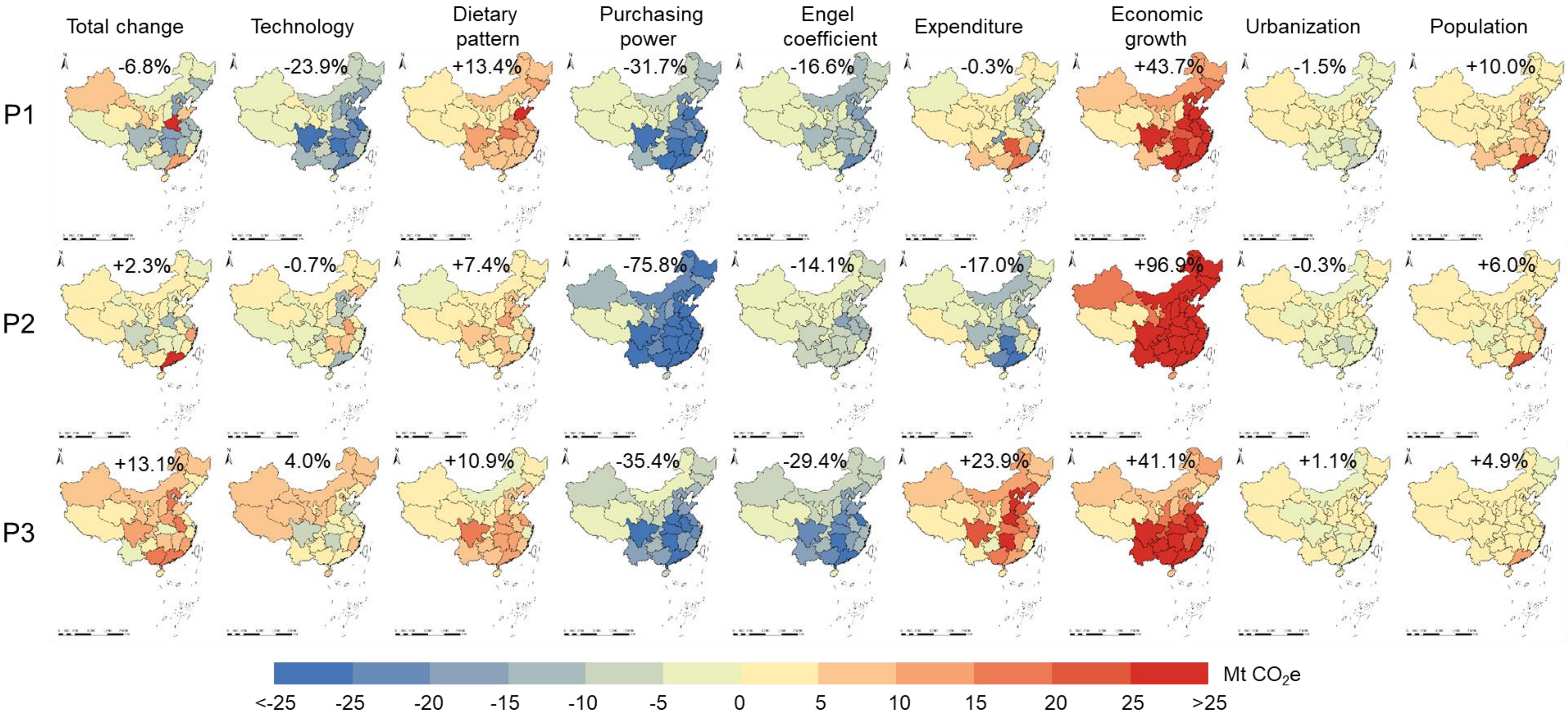

Figure 6 Spatial patterns in total food system GHGs emissions changes in China and the role of eight drivers between 1990 and 2018. Percentage values indicate the contribution made by each driver to overall. P1, P2 and P3 represent the periods of 1990-2000,2000-2010, and 2010-2018, respectively.

3.4 Regional coupling trends of food system emissions and economic growth

Economic growth has been identified as the most significant determinant of regional consumption-based FSE. However, the impact of economic growth varies across different regions, leading to shifting trends in the coupling patterns between carbon emissions in food systems and economic growth. Specifically, two quadrants can be identified (Fig. 7): (1) the Coupling Quadrant, characterized by economically-driven emission growth, where high emissions were coupled with high economic development, such that increases in food system emissions occurred alongside economic growth; (2) the Decoupling Quadrant, indicative of sustainable development, where economic growth was achieved concurrently with reductions in food system emissions.

Most regions initially followed a decoupling development pattern in P1 (i.e. 1990–2000). This sustainable transition can be largely attributed to improvements in production efficiency, in particular the reduction of energy-intensive food production practices using coal, despite the expansion in meat-dominated diets. In the promotion of economic growth, the South China and Northeast regions were the first to transition from the decoupling quadrant to the coupling quadrant during P2 (2000–2010). This shift mirrors the national average, where, in most areas, the drivers of economic growth and consumer expenditure facilitated the transition to the coupling quadrant in P3 (2010–2018). Moreover, in the southern regions, especially EC, CC, SC, and SW, this transition was significantly influenced by the transformation of the consumption structure towards high carbon density.

Therefore, regions with high FSE but persistently high economic levels need to decouple FSE from economic growth. Conversely, regions currently in a sustainable development model should avoid transitioning to unsustainable patterns with regional specific strategies. At the national level, pricing mechanisms for high carbon-intensive foods, coupled with the promotion of low-carbon and healthy dietary guidelines should be implemented. Regionally there is an urgent need to expedite dietary shifts, particularly in the economically developed southern regions. Concurrently, in northern regions, which are predominantly food-producing areas, the adoption of sustainable agricultural practices is essential to enhance the potential for emission reduction through technological effects.

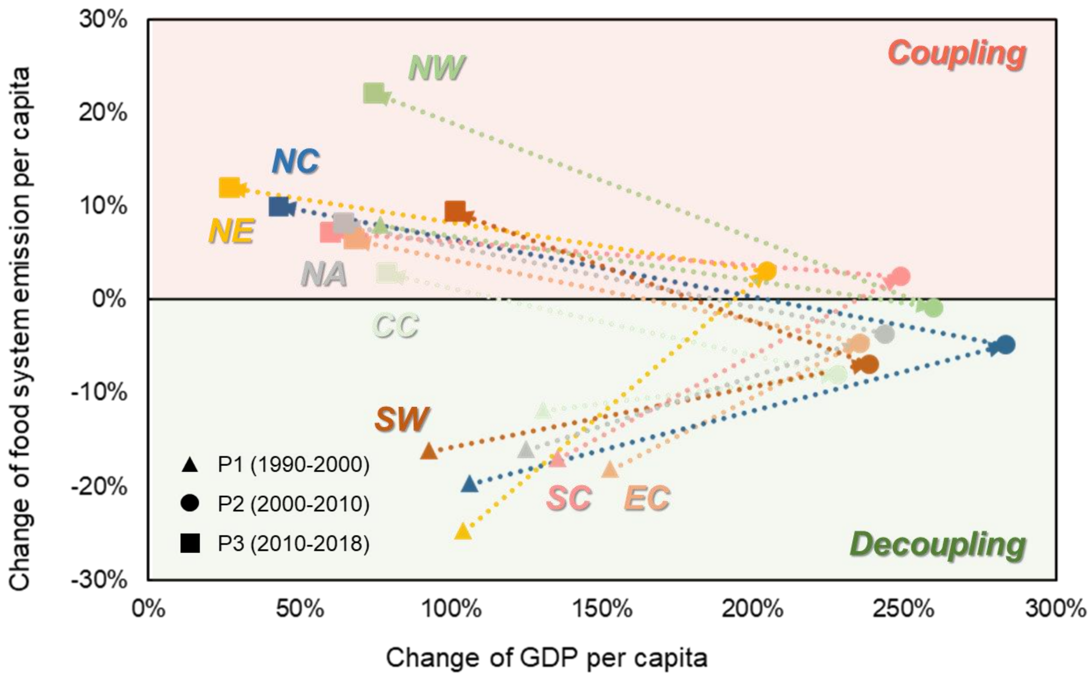

Figure 7 Decoupling and coupling trends in per capita food system GHGs and per capita GDP from seven regions in China.

4. Discussion

In this study, a provincial food type-specific "bottom-up" GHGs inventory of China's food system enables an exploration of regional downscaling for food system emission accounting and driver decomposition. This investigation addresses the significant gap in regional lifecycle emission estimations and driver differentiation within the country's food systems. Our results indicate that the diminished use of raw coal in the production stage for cereals in East, Central, and Southwest China was a significant driver of reductions in food system GHG emissions between 1990 and 2000 (Fig. S1 and S2). This finding aligns with the conclusions drawn by He et al. (2021), and further extends the spatial disaggregation of food system emissions, emphasizing that technical progress remains a dominant force in mitigating dietary GHG emissions. However, as the food supply chains have evolved, post-production stages have demonstrated increasing reliance on energy (Tubiello et al., 2021), necessitating a transition towards cleaner energy supplies to counteract the impacts of energy-dependent food supply chains. Consistent with Garnett and Wilkes (2014), but integrating regional details, this study identifies economic growth as the preeminent factor driving increases in China’s food system GHGs, especially in East, Central, South, and Southeast regions. The swift growth rate of China's FSE since 2010 has predominantly been propelled by surges in consumer expenditure in Central, East, and North China, coupled with transitions in dietary patterns. These patterns are principally associated with GHG-intensive meat and protein foods, especially in the more developed areas of East, Central, Southwest, and South China.

This study not only identifies regional variations in FSE but also examines the disparate impacts of various drivers across regions. Such insights are instrumental in shaping region-specific mitigation policies, particularly for developed areas. Notably, our findings highlight that the most significant factors at the national level — economic growth and purchasing power — are predominantly concentrated in the developed southern regions of China, contributing to approximately 83.7% of FSE in the most recent period (P3; 2010–2018; Fig. 5e). These regions are also experiencing rapid economic growth, contributing to 77.3% of China's GDP (NSB, 2021). Additionally, extant research corroborates that regions with higher incomes have greater potential for emission reductions through shifts in dietary patterns (Sun et al., 2022). Adding to the existing literature, our findings suggest that the FSE driven by economic growth in China's developed areas will persist in exerting pressure on efforts to mitigate these emissions (Fig. 7). Consequently, developing differentiated food system reduction policies that take into account regional development levels is of paramount importance.

Currently, a preponderance of food system policies are predominantly oriented towards the supply side, with inadequate attention to regionally differentiated compensation strategies. Specifically, 45% of all policies focus on Land Use, Land-Use Change, and Forestry (LULUCF) and production stages, whereas a mere 10% are consumption-oriented Cerutti et al. (2023). Furthermore, not every one of these policies sufficiently addresses their potential environmental impacts (Cerutti et al., 2023). The role of food prices as a pivotal instrument in modulating environmentally sustainable consumption behaviors has been well-established from the demand side (Latka et al., 2021). This study also posits that the price elasticity of food could significantly contribute to national emission mitigation strategies (Fig. 4). Frank et al. (2019) have suggested that a well-implemented food carbon tax policy holds the potential to reduce global GHGs by approximately 8% by 2050. However, the implementation of carbon tax policies in the food sector necessitates meticulous consideration to circumvent, inducing food insecurity among less developed areas and low-income groups. This is imperative as the food demand of lower-income groups is typically price-inelastic, and a carbon tax on agricultural GHG emissions escalates production costs, contingent on the GHG intensity of production. Consequently, any redistributive mechanisms employed should be attuned to regional disparities and be designed to avert the risks of hunger and malnutrition that could emanate from spatially uniform emission mitigation policies (Hasegawa et al., 2018; Soergel et al., 2021).

The uncertainty analysis in this study follows the IPCC Guidelines for National Greenhouse Gas Inventories for good practices and uncertainty management (IPCC, 2006) (see Supplementary Information). Uncertainties in the emissions from the production stage of the food lifecycle mainly come from regional differences in activity survey data collected in the production process (for example, those describing fertilizer and energy use). The uncertainties in the processing and retail stages are primarily derived from the emission factors in the literature or the LCA database. Uncertainties in the transportation stage mainly come from the spatial allocation of food transport emissions by rail and road based on transport statistical data. The surveyed consumption activity data for different regions are the main source of uncertainties for the consumption stage.

Concurrent with numerous studies, the present research acknowledges certain limitations. Due to the sectoral precision constraints inherent in Multi-Regional Input-Output (MRIO) tables, inter-regional emission transfers were not integrated into our computations. Subsequent research endeavors will employ food type-specific MRIO models to refine calculations of embodied emissions across regions (Ye et al., 2022), thereby elucidating consumption-based inter-regional emission responsibilities with greater clarity. The established food system framework disrupts traditional sectoral categories found within the national GHG inventory framework as outlined by the IPCC (2006) (Rosenzweig et al., 2020). However, the evolution of understanding necessitates the development of innovative practical frameworks for assessing food system GHGs (IPCC, 2019). In light of the rapid progression of food supply chains (Garnett, 2011) and the escalating imperative for such chains to adapt to climate change (Gustafson et al., 2021), emissions related to supply chain have been incrementally incorporated into food system emission accounting (Crippa et al., 2021; Fan, 2021; Fei et al., 2020). Nevertheless, existing policies targeting the mitigation of food system impacts during post-production stages remain notably scarce, with consumption-oriented policies comprising only 10% of the total, alongside transport at 2%, processing at 2%, and retail at 2% (Cerutti et al., 2023). This study thus underscores the need for heightened focus on consumer-end management and the strategic optimization of the spatial configuration of food supply chains to actualize emissions reduction within the food system.

Emission accounting largely depends on the system boundaries (Tubiello et al., 2021). If land use changes are considered only, the current results will be slightly underestimated. The carbon emissions caused by land use changes in China were approximately 3.8 Mt CO_2e in 2015, accounting for about 0.2% of the total emissions from the food system (Crippa, et al., 2021). Additionally, statistics from FAOSTAT suggests emissions of 6.3 Mt CO_2e from biomass burning, and 4.9 Mt CO_2e from land drained for agriculture. However, if the forest carbon sink is also taken into account, the results will be greatly overestimated, as the FAOSTAT data indicates -711.8 Mt CO_2e from forest carbon sinks. Additionally, it is difficult to separate the changes caused by people direct consumption and for animal feed, and to allocate these to different crop types. Therefore, this study excludes the carbon emissions caused by land use changes. Furthermore, recent studies have quantified the emissions from food loss and waste within China's life cycle at the national scale, using material flow methods. These emissions are estimated to be approximately 390.4 Mt CO_2e (Zhu et al., 2023) and 464 Mt CO_2e (Xue et al., 2021). Evaluating food loss and waste depend on research into regional supply chain processes, but this study does not cover them. In this study, the major efforts have been expended on identifying an array of parameters that possess temporal and spatial comparability to suit the requirements of LCA. However, due to the limitations in data availability, uncertainties have emerged in the calculation of average values for representative food types.

To facilitate the quantitative attribution of factors, we selected the Logarithmic Mean Divisia Index (LMDI) method for its advantages in handling negative values flexibly and eliminating residual terms (Ang, 2005). Like all methodologies, LMDI operates under certain assumptions. These include the assumption of perfect divisibility, the lack of accounting for statistical significance, and the potential for interactivity among decomposed factors, since inter-relationships are inherent aspect of the decomposition process (Ang, 2015). Future research will build upon the results of the LMDI decomposition by adjusting decomposed factors and employing other attribution analysis methods, such as the Shapley Value Regression (Aras and Van, 2022). These approaches aim to further elucidate the underlying mechanisms of influence enabling a refinement of our understanding of the complex interplays within the factors influencing FSE in China.

5. Conclusion

By constructing a regional specific bottom-up food system emission inventory with food type details, this study employs the decomposition analysis method to dissect the transformation trends of food system emissions in China, subsequently downscaling drivers to the provincial level. China's food system emissions initially decline over the period of 1990–2000. This was followed by a surge in emissions that were primarily concentrated in the southern region. Within East, Central, and Southwest China, optimization of the food system's energy structure by reducing coal for food production resulted in emissions declines before 2000. The subsequent increase can primarily be attributed to a combination of economic growth, consumer expenditure, and shift in dietary pattern, factors which are more pronounced in the developed southern regions. FSE in developed regions have long been driven by economic growth.

This research identifies the distinct characteristics, and spatiotemporal drivers, of emissions within China's food system. It concludes that the implementation of regionally differentiated mitigation policies is imperative to curtail food system emissions with particular potential related to guiding dietary shifts and instituting regionally differentiated pricing policies in developed regions. Furthermore, the study emphasizes the significance of regional offset mechanisms for food system emission and a concerted focus on the lifecycle carbon management of the food system.

References

Ang, B. W. (2004). Decomposition analysis for policymaking in energy:: which is the preferred method?. Energy policy, 32(9), 1131-1139.

Acampora, A., Ruini, L., Mattia, G., Pratesi, C.A., Lucchetti, M.C., 2023. Towards carbon neutrality in the agri-food sector: Drivers and barriers. Resources, Conservation and Recycling 189, 106755.

Aras, S., & Van, M. H. (2022). An interpretable forecasting framework for energy consumption and CO_2 emissions. Applied Energy, 328, 120163.

Bajželj, B., Richards, K.S., Allwood, J.M., Smith, P., Dennis, J.S., Curmi, E., Gilligan, C.A., 2014. Importance of food-demand management for climate mitigation. Nature Climate Change 4(10), 924-929.

Cerutti, N., Lamb, W.F., Crippa, M., Leip, A., Solazzo, E., Tubiello, F.N., Minx, J.C., 2023. Food system emissions: a review of trends, drivers, and policy approaches, 1990-2018. Environmental Research Letters.

Chen, X., Cui, Z., Fan, M., Vitousek, P., Zhao, M., Ma, W., Wang, Z., Zhang, W., Yan, X., Yang, J., 2014. Producing more grain with lower environmental costs. Nature 514(7523), 486-489.

Crippa, M., Solazzo, E., Guizzardi, D., Monforti-Ferrario, F., Tubiello, F.N., Leip, A., 2021. Food systems are responsible for a third of global anthropogenic GHG emissions. Nature Food 2(3), 198-209.

Duan, Y., Gao, Y., Zhao, J., Xue, Y., Zhang, W., Wu, W., Jiang, H., Cao, D., 2023. Agricultural Methane Emissions in China: Inventories, Driving Forces and Mitigation Strategies. Environmental Science & Technology.

EU, 2020. Farm to Fork Strategy. https://ec.europa.eu/food/farm2fork_en.

Fan, S., 2021. Economics in food systems transformation. Nature Food 2(4), 218-219.

FAOSTAT, 2023. Detailed trade matrix, Food and agriculture data, in: FAO (Ed.).

Fei, S., Ni, J., Santini, G., 2020. Local food systems and COVID-19: an insight from China. Resources, conservation, and recycling 162, 105022.

Frank, S., Havlík, P., Stehfest, E., van Meijl, H., Witzke, P., Pérez-Domínguez, I., van Dijk, M., Doelman, J.C., Fellmann, T., Koopman, J.F., 2019. Agricultural non-CO2 emission reduction potential in the context of the 1.5° C target. Nature Climate Change 9(1), 66-72.

Fujimori, S., Wu, W., Doelman, J., Frank, S., Hristov, J., Kyle, P., Sands, R., Van Zeist, W.-J., Havlik, P., Domínguez, I.P., 2022. Land-based climate change mitigation measures can affect agricultural markets and food security. Nature Food 3(2), 110-121.

Gao, B., Huang, W., Wang, L., Huang, Y., Ding, S., Cui, S., 2019. Driving forces of nitrogen flows and nitrogen use efficiency of food systems in seven Chinese cities, 1990 to 2015. Science of the Total Environment 676, 144-154.

Garnett, T., 2011. Where are the best opportunities for reducing greenhouse gas emissions in the food system (including the food chain)? Food policy 36, S23-S32.

Garnett, T., Wilkes, A., 2014. Appetite for change: social, economic and environmental transformations in China’s food system. Food Climate Research Network.

Godfray, H.C.J., Aveyard, P., Garnett, T., Hall, J.W., Key, T.J., Lorimer, J., Pierrehumbert, R.T., Scarborough, P., Springmann, M., Jebb, S.A., 2018. Meat consumption, health, and the environment. Science 361(6399), eaam5324.

Godfray, H.C.J., Beddington, J.R., Crute, I.R., Haddad, L., Lawrence, D., Muir, J.F., Pretty, J., Robinson, S., Thomas, S.M., Toulmin, C., 2010. Food security: the challenge of feeding 9 billion people. science 327(5967), 812-818.

Gustafson, D., Asseng, S., Kruse, J., Thoma, G., Guan, K., Hoogenboom, G., Matlock, M., McLean, M., Parajuli, R., Rajagopalan, K., 2021. Supply chains for processed potato and tomato products in the United States will have enhanced resilience with planting adaptation strategies. Nature Food 2(11), 862-872.

Hasegawa, T., Fujimori, S., Havlík, P., Valin, H., Bodirsky, B.L., Doelman, J.C., Fellmann, T., Kyle, P., Koopman, J.F., Lotze-Campen, H., 2018. Risk of increased food insecurity under stringent global climate change mitigation policy. Nature Climate Change 8(8), 699-703.

Hayek, M.N., Harwatt, H., Ripple, W.J., Mueller, N.D., 2021. The carbon opportunity cost of animal-sourced food production on land. Nature Sustainability 4(1), 21-24.

He, P., Baiocchi, G., Hubacek, K., Feng, K., Yu, Y., 2018. The environmental impacts of rapidly changing diets and their nutritional quality in China. Nature Sustainability 1(3), 122-127.

He, P., Feng, K., Baiocchi, G., Sun, L., Hubacek, K., 2021. Shifts towards healthy diets in the US can reduce environmental impacts but would be

unaffordable for poorer minorities. Nature Food 2(9), 664-672.
Heller, M.C., Keoleian, G.A., 2015. Greenhouse gas emission estimates of US dietary choices and food loss. Journal of Industrial Ecology 19(3), 391-401.
Hong, C., Burney, J.A., Pongratz, J., Nabel, J.E., Mueller, N.D., Jackson, R.B., Davis, S.J., 2021. Global and regional drivers of land-use emissions in 1961–2017. Nature 589(7843), 554-561.
Huang, W., Gao, B., Lin, J., Cui, S., Zhong, Q., Huang, C., 2020. Driving forces of nitrogen input into city-level food systems: Comparing a food-source with a food-sink prefecture-level city in China. Resources, Conservation and Recycling 160, 104850.
IPCC, 2006. IPCC Guidelines for National Greenhouse Gas Inventories.
IPCC, 2019. Climate change and land: an IPCC special report on climate change, desertification, land degradation, sustainable land management, food security, and greenhouse gas fluxes in terrestrial ecosystems.
IPCC, 2022. Mitigation of Climate Change, IPCC Six Assessment Report, Climate Change 2022.
Kehlbacher, A., Tiffin, R., Briggs, A., Berners-Lee, M., Scarborough, P., 2016. The distributional and nutritional impacts and mitigation potential of emission-based food taxes in the UK. Climatic Change 137, 121-141.
Kramer, K.J., Moll, H.C., Nonhebel, S., Wilting, H.C., 1999. Greenhouse gas emissions related to Dutch food consumption. Energy policy 27(4), 203-216.
Lai, L., Huang, X., Yang, H., Chuai, X., Zhang, M., Zhong, T., Chen, Z., Chen, Y., Wang, X., Thompson, J.R., 2016. Carbon emissions from land-use change and management in China between 1990 and 2010. Science Advances 2(11), e1601063.
Latka, C., Kuiper, M., Frank, S., Heckelei, T., Havlík, P., Witzke, H.-P., Leip, A., Cui, H.D., Kuijsten, A., Geleijnse, J.M., 2021. Paying the price for environmentally sustainable and healthy EU diets. Global Food Security 28, 100437.
Li, Y., Wang, L.-e., Liu, G., Cheng, S., 2021. Rural household food waste characteristics and driving factors in China. Resources, Conservation and Recycling 164, 105209.
Liu, G., Zhang, F., & Deng, X. 2023. Half of the greenhouse gas emissions from China’s food system occur during food production. Communications Earth & Environment, 4(1), 1-13.
Poore, J., Nemecek, T., 2018. Reducing food’s environmental impacts through producers and consumers. Science 360(6392), 987-992.
Qi, X., Feng, K., Sun, L., Zhao, D., Huang, X., Zhang, D., Liu, Z., Baiocchi, G., 2022. Rising agricultural water scarcity in China is driven by expansion of irrigated cropland in water scarce regions. One Earth 5(10), 1139-1152.

Qi, X., Huang, X., Song, Y., Wang, D., Zhong, T., Liu, Z., 2023. Grain carbon emission transfer and its spatiotemporal shifts based on the increasing supply-demand separation in China over the past three decades. Science China Earth Sciences, 1-21.

Qiang, Q., Jian, C., 2020. Natural resource endowment, institutional quality and China's regional economic growth. Resources Policy 66, 101644.

Ren, M., Huang, C., Wu, Y., Deppermann, A., Frank, S., Havlík, P., Zhu, Y., Fang, C., Ma, X., Liu, Y., 2023. Enhanced food system efficiency is the key to China’s 2060 carbon neutrality target. Nature food, 1-13.

Roe, S., Streck, C., Obersteiner, M., Frank, S., Griscom, B., Drouet, L., Fricko, O., Gusti, M., Harris, N., Hasegawa, T., 2019. Contribution of the land sector to a 1.5 C world. Nature Climate Change 9(11), 817-828.

Rosenzweig, C., Mbow, C., Barioni, L.G., Benton, T.G., Herrero, M., Krishnapillai, M., Liwenga, E.T., Pradhan, P., Rivera-Ferre, M.G., Sapkota, T., 2020. Climate change responses benefit from a global food system approach. Nature Food 1(2), 94-97.

Schierhorn, F., Kastner, T., Kuemmerle, T., Meyfroidt, P., Kurganova, I., Prishchepov, A.V., Erb, K.-H., Houghton, R.A., Müller, D., 2019. Large greenhouse gas savings due to changes in the post-Soviet food systems. Environmental Research Letters 14(6), 065009.

Soergel, B., Kriegler, E., Bodirsky, B.L., Bauer, N., Leimbach, M., Popp, A., 2021. Combining ambitious climate policies with efforts to eradicate poverty. Nature Communications 12(1), 2342.

Sun, M., Chen, G., Xu, X., Zhang, L., Hubacek, K., Wang, Y., 2021. Reducing carbon footprint inequality of household consumption in rural areas: analysis from five representative provinces in China. Environmental science & technology 55(17), 11511-11520.

Sun, Z., Scherer, L., Tukker, A., Spawn-Lee, S.A., Bruckner, M., Gibbs, H.K., Behrens, P., 2022. Dietary change in high-income nations alone can lead to substantial double climate dividend. Nature Food 3(1), 29-37.

Tubiello, F.N., Karl, K., Flammini, A., Gütschow, J., Obli-Layrea, G., Conchedda, G., Pan, X., Qi, S.Y., Heiðarsdóttir, H.H., Wanner, N., 2022. Pre-and post-production processes along supply chains increasingly dominate GHG emissions from agri-food systems globally and in most countries. Earth System Science Data Discussions, 1-24.

Tubiello, F.N., Rosenzweig, C., Conchedda, G., Karl, K., Gütschow, J., Xueyao, P., Obli-Laryea, G., Wanner, N., Qiu, S.Y., De Barros, J., 2021. Greenhouse gas emissions from food systems: building the evidence base. Environmental Research Letters 16(6), 065007.

Wang, Q., & Su, M. 2020. Drivers of decoupling economic growth from carbon emission–an empirical analysis of 192 countries using decoupling model and decomposition method. Environmental Impact Assessment Review, 81,

106356.
Xing, L., Lin, T., Hu, Y., Lin, M., Liu, Y., Zhang, G., Ye, H., Xue, X., 2023. Reducing food-system nitrogen input and emission through circular agriculture in montane and coastal regions. Resources, Conservation and Recycling 188, 106726.
Xue, L., Liu, X., Lu, S., Cheng, G., Hu, Y., Liu, J., Dou, Z., Cheng, S., Liu, G., 2021. China’s food loss and waste embodies increasing environmental impacts. Nature Food 2(7), 519-528.
Yang, H., Huang, X., Hu, J., Thompson, J. R., Flower, R. J. 2022. Achievements, challenges and global implications of China’s carbon neutral pledge. Frontiers of Environmental Science & Engineering, 16(8):111. DOI:10.1007/s11783-022-1532-9
Ye, Q., Bruckner, M., Wang, R., Schyns, J.F., Zhuo, L., Yang, L., Su, H., Krol, M.S., 2022. A hybrid multi-regional input-output model of China: Integrating the physical agricultural biomass and food system into the monetary supply chain. Resources, conservation and recycling 177, 105981.
Zhang, H., Xu, Y., Lahr, M.L., 2022. The greenhouse gas footprints of China's food production and consumption (1987–2017). Journal of Environmental Management 301, 113934.
Zhang, W., Dou, Z.-x., He, P., Ju, X.-T., Powlson, D., Chadwick, D., Norse, D., Lu, Y.-L., Zhang, Y., Wu, L., 2013. New technologies reduce greenhouse gas emissions from nitrogenous fertilizer in China. Proceedings of the National Academy of Sciences 110(21), 8375-8380.
Zhang, Y., Fan, S., Chen, Z., Feng, X., Zhang, X., Bai, Z., Wang, X. 2021. Transforming agri-food systems to help achieve China's 2060 carbon neutrality goal. China and Global Food Policy Report: 12-23. https://agfep.cau.edu.cn/module/download/downfile.jsp?classid=0&filename=2104301731175261.pdf
Zhao, H., Chang, J., Havlík, P., van Dijk, M., Valin, H., Janssens, C., Ma, L., Bai, Z., Herrero, M., Smith, P., 2021. China’s future food demand and its implications for trade and environment. Nature Sustainability 4(12), 1042-1051.